

CE 595 - PROJECT 2:
CHARACTERIZATION OF THE MODE I FRACTURE ENERGY OF ADHESIVE
JOINTS

FERNANDO DRI
DAVID RESTREPO

Instructor
PROF. PABLO D. ZAVATTIERI

PURDUE UNIVERSITY
SCHOOL OF ENGINEERING
CIVIL ENGINEERING
SPRING – 2011

TABLE OF CONTENTS

1. INTRODUCTION	3
2. PROBLEM DESCRIPTION	3
3. METHODOLOGY	3
1. Adhesive bounded double cantilever beam (DCB) test	3
2. Numerical simulations	5
a. General cohesive model	5
b. Abaqus simulations	7
c. FEAP simulations.....	10
d. Comparison between Abaqus and FEAP simulations.....	13
4. DISCUSSION	13
5. FUTURE WORK.....	14
ACNOWLEDGMENTS	14
REFERENCES	14
APPENDIX 1: FEAP DISCREPANCY	15

1. INTRODUCTION

The use of adhesive joints has been growing steadily in recent years. The said practice bears some major advantages over other methods. Among these are the possibility to join dissimilar materials and the ability to absorb residual strains created as a result of thermal stresses, their high strength-to-weight ratio, low cost, etc. As the use of adhesive joints in structural parts becomes more frequent, the need to define rigorous failure criteria becomes more crucial^[1].

The concepts of fracture mechanics have been widely employed in studies concerned with crack growth in adhesive joints. Of the various test specimens that have been used to measure the adhesive fracture energy, the double-cantilever beam (DCB) specimen, has been one of the most popular^[2].

The outline of the rest of the report is as follows: Section 2 presents the problem description. Section 3 presents the methodology used to characterize the fracture energy of the adhesive. Section 4 presents a short discussion on the founded results and finally section 5 presents the future work.

2. PROBLEM DESCRIPTION

The aim of this project is to characterize the Mode I fracture energy of a commercial adhesive using experimental data and a CZM approach. To obtain the cohesive law of the adhesive, experiments will be carried out on a double cantilever beam specimen made of steel bounded with Loctite 415 (particularly suited to bonding of metal substrate). The results of the experiment will be fitted using numerical simulations.

3. METHODOLOGY

1. Adhesive bounded double cantilever beam (DCB) test

Six bounded double cantilever beam (DBC) specimens schematically shown in Figure 1 were fabricated using steel (SAE 1018) and commercial adhesive (Loctite 415). The total length of the steel beams was 300 mm and the width was 25.4 mm. Three of the specimens were fabricated using a thickness of 3 mm and the other three with a thickness of 6mm for the steel arms. The thickness of the adhesive was kept at 0.05 mm for all tests. The initial crack length (Precrack) was defined to be 55 mm. Door hinges were bonded to the free ends of the specimen to transmit the load to the specimen during the test (Figure 2).

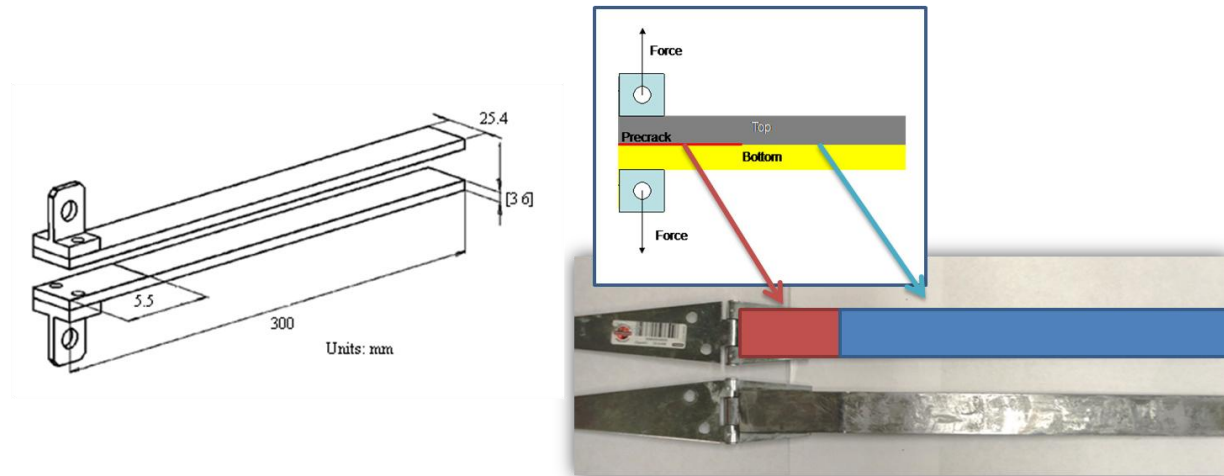


Figure 1: Double cantiliver beam (DCB) specimen: Two beams of steel 1018 bounded with Loctite 415. Precrack length: 55 mm.

The test was performed using a testing machine under displacement control at nominal cross head displacement rate of 1 mm/s. The assembly for the test is presented on Figure 2.

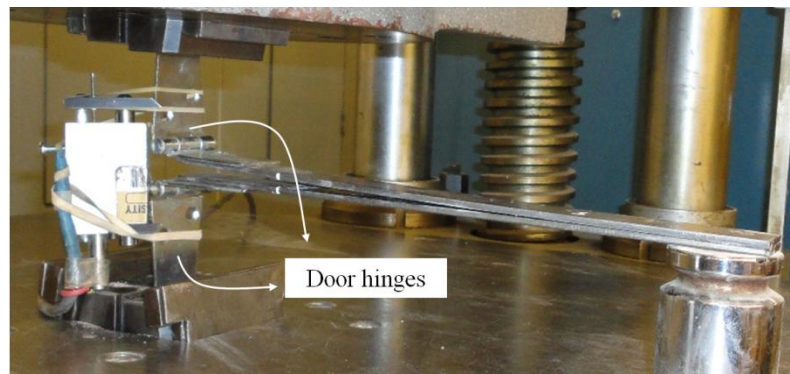


Figure 2: Assembly for test. Bonded door hinges are used to transmit the load from the testing machine to the specimen.

Load-displacement curves for the test are presented on Figure 3. The curves labeled with a B at the end, represents the specimens with a steel arm of 6mm, the other curves are for the DCB specimens with a steel arm of 3 mm. As it is observed on the figure, the curves obtained for the specimens with an arm thick of 3mm present an estrange behavior due to the sensibility of the testing machine that is much more inferior than the resistance of these specimens. The lower measurable value of the testing machine is 500 N.

Despite that the lower measurable value of the testing machine is also higher than the resistance founded for the specimens with an arm thickness of 6 mm, the load-displacement curves founded for these specimens follow approximately the expected behavior for a DCB test (Figure 13-appendix) and for that reason these curves are used to characterize the fracture energy of the adhesive and the cohesive model for the numerical simulations.

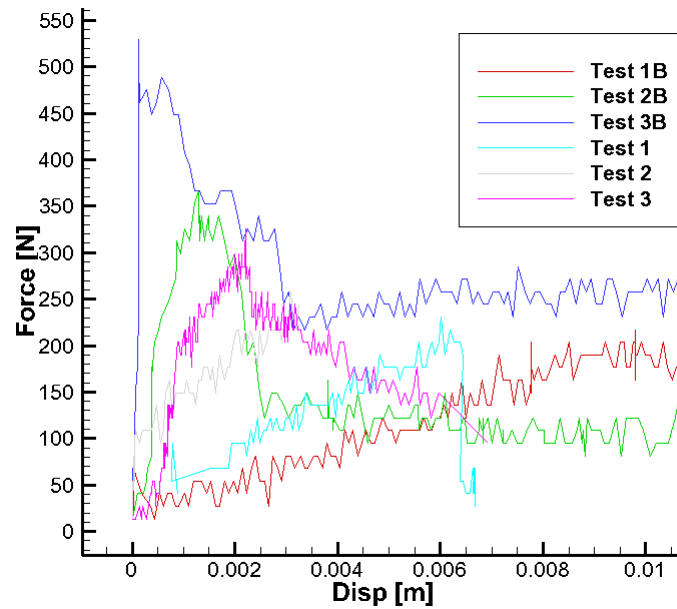


Figure 3: Load-Displacement curves for the DCB test. Curves label with a B at the end represents the test DCB specimens with a steel arm of 6mm, the other curves are for the DCB specimens with a steel arm of 3 mm.

2. Numerical simulations

a. General cohesive model

Using the data obtained from experiments and LEFM it is possible to calculate an initial value for the fracture energy. This first result is going to be used to estimate an order of magnitude for the energy and as an initial guess for the cohesive law used in the simulations. The cohesive law is defined using a triangular law (Figure 4.)

The fracture energy can be obtained from:

$$(1) G = \frac{12 \times P^2 \times a^2}{E \times h^3 \times B^2} = 348 \text{ N/m} \quad (1)$$

Where P is 530 N and correspond to the maximum load founded from the tests, a is 0.055 m and correspond to the precrack length, h is the height of the samples ($h = 0.006$ m) and B is the width of the samples ($B = 0.0254$ m)

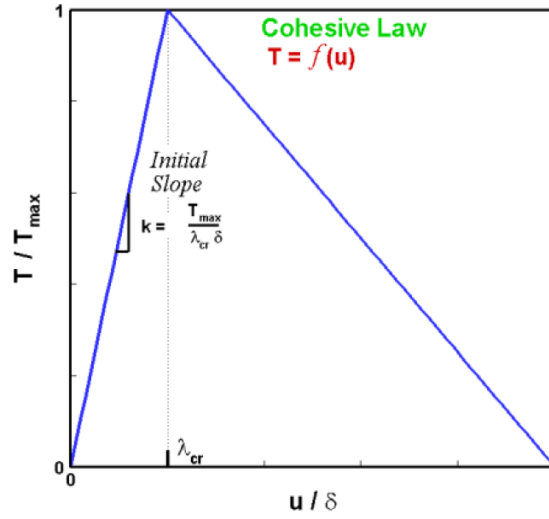


Figure 4: Triangular law used to represent the cohesive behavior.

Defining T_{max} as 12 MPa based on the data sheet of the adhesive and with the shape of the cohesive law it is possible to obtain δ_c

$$\delta_c = \frac{2 \times G}{T_{max}} \rightarrow \delta_c = 5.8e^{-5} \text{ m} \quad (2)$$

The fracture process zone length can be approximated as:

$$l_{FPZ} \approx E_{adh} \times \frac{G}{T_{max}^2} \rightarrow l_{FPZ} = 0.0145 \text{ m} \quad (3)$$

Where E_{adh} is equal to 6 GPa^[3].

Considering approximately 10 elements inside the fracture process zone we define $h = 1 \text{ mm}$ as the representative size of the final element mesh.

To avoid instabilities problems the initial stiffness of the cohesive law should be much greater than the bulk element. The following equations will define the final shape of the triangular law^[4]:

$$K = 10 \times \frac{E}{h} \rightarrow K = 2.1e^{15} \text{ Pa/m} \quad (4)$$

Where E is the Young modulus of the arms of the DCB ($E=210e^9$ Pa) and h is the length of the cohesive elements ($h = 0.001$ m).

Finally the λ_{cr} is estimated using:

$$\lambda_{cr} = \frac{T_{\max}}{\delta_c \times K} \rightarrow \lambda_{cr} = 9.85e^{-5} \quad (5)$$

b. Abaqus simulations

The general cohesive model founded on the previous section is calibrated using numerical simulations in the finite element software Abaqus. The procedure used to model the DCB test in Abaqus is summarized on Figure 5. The steel arms of the beam are meshed using 4 node quadrilateral plane strain elements; while the adhesive is modeled using user defined cohesive elements. The length of the cohesive elements is 1 mm in order to obtain at least 10 elements on the fracture process zone. The simulation is made using the Standard solver with an adaptive incremental scheme.

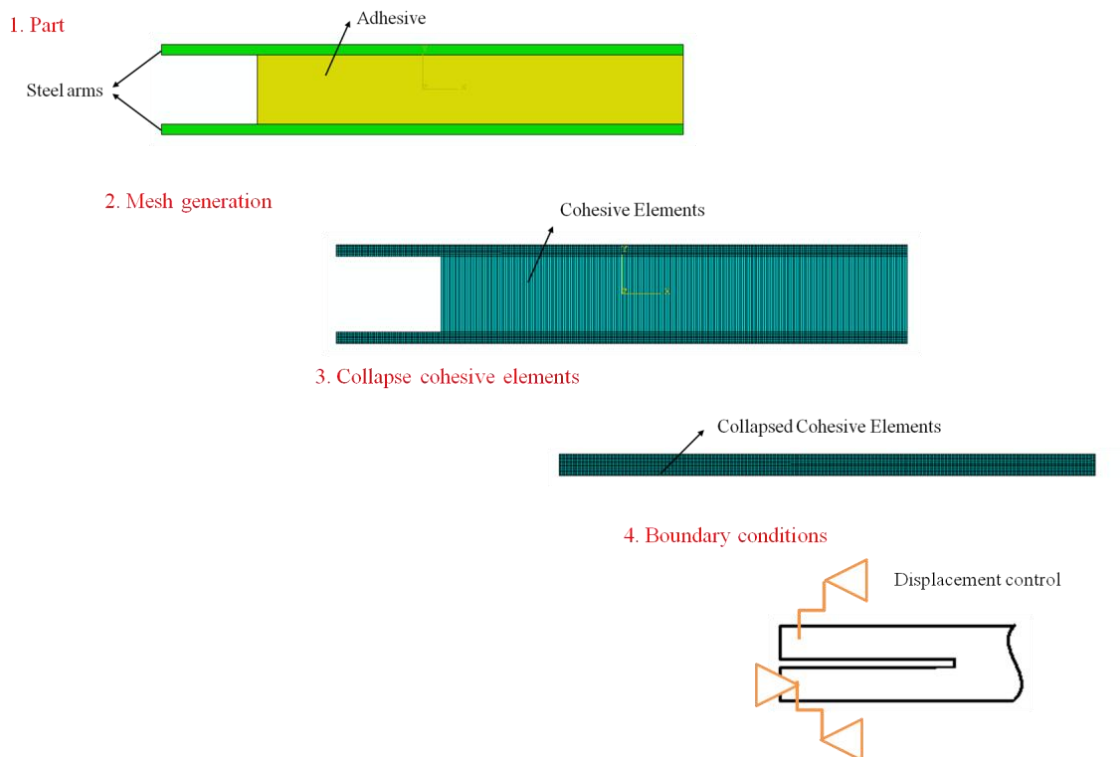


Figure 5: Procedure followed in abaqus simulations for the DCB test.

Using the simulations it is explored the effect of T_{max} and G on the cohesive model.

Effect of T_{max}

To capture the effect of T_{max} over the system, the following analyses were conducted:

Table 1: Cases analyzed to capture the influence of T_{max} on the cohesive model

G	T max	δ_c	λ
[J/m ²]	[MPa]	[m]	[dimensionless]
348	8	8.70E-05	4.38E-05
348	12	5.80E-05	9.85E-05
348	16	4.35E-05	1.75E-04
348	20	3.48E-05	2.74E-04
348	24	2.90E-05	3.94E-04

Figure 6, presents a study of the effect of T_{max} on the cohesive model. Contrary at it was expected, there is a variation on the behavior of the simulated specimen influenced by changes in T_{max} ; also there is an expected variation on the initial slope on the Force-Displacement curves that does not reflect the behavior of the triangular cohesive law.

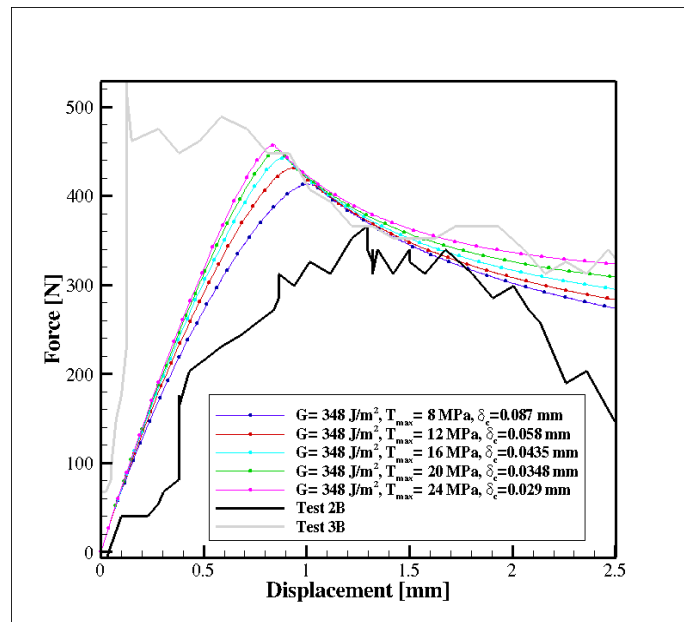


Figure 6: Influence of T_{max} on the cohesive model (Abaqus)

Effect of G

To capture the effect of G over the system, the following analyses were conducted:

Table 2: Cases analyzed to capture the influence of G in the cohesive model

G	T_{max}^1	δ_c	λ
[J/m ²]	[MPa]	[m]	[dimensionless]
200	16	2.50E-05	3.05E-04
300	16	3.75E-05	2.03E-04
400	16	5.00E-05	1.52E-04
500	16	6.25E-05	1.22E-04

Figure 7, presents a study of the effect of G on the cohesive model. As it was expected, when we increase G , there is an increase on the maximum peak load of the system; but also there is an unexpected change of the initial slope on the Force-Displacement curves that does not reflect the behavior of the triangular cohesive law.

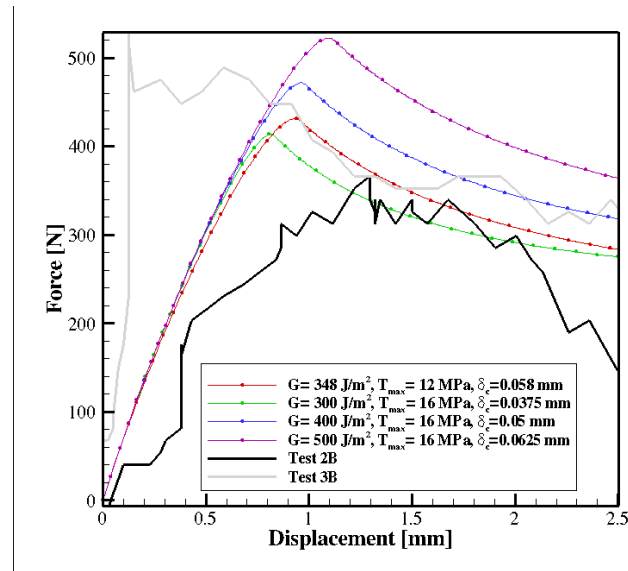


Figure 7: Influence of G in the cohesive model (Abaqus)

From Figure 6 and Figure 7, we can appreciate that the initial educated guess of the parameters that define the cohesive model ($T_{max} = 12$ MPa, and $G = 348$ J/m²), was consequent with the experimental test.

¹ The value of 16MPa for T_{max} was chosen because it is in the middle of the analyzed range.

c. FEAP simulations

These analyses were done to contrast Abaqus results. Both the model and cohesive law are quite similar, being the solving scheme the only change. For these simulations an explicit solver with a fixed timestep was used.

To keep the same characteristics as Abaqus a mesh generator was coded up for FEAP to create the DCB specimen and add cohesive elements inside it.

Finding the “optimal” speed

When an explicit scheme is used the simulated testing speed becomes an important parameter. In this case a quick evaluation was made using speeds ranging from 1m/s to 1 mm/s.

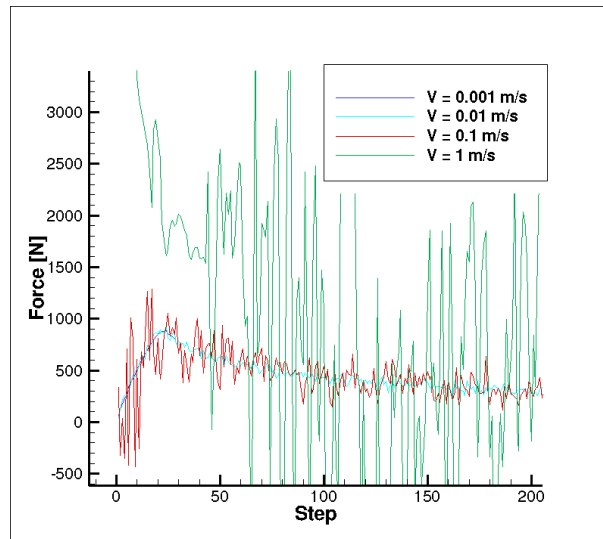


Figure 8: Force vs Timestep for different pulling speeds

Ideally 1 mm/s would be the best possible solution but the necessary time is too high (more than 5 days for each simulation). A value of 10 mm/s was adopted.²

The timestep was fixed to $1e^{-5}$ ms.

² Mass scaling was proposed by professor Zavattieri to reduce the computational time. At the time of writing this report all the analyses were already done. Because of that the option was not used.

Effect of T_{max}

The analyses characteristics are explained in Table 1.

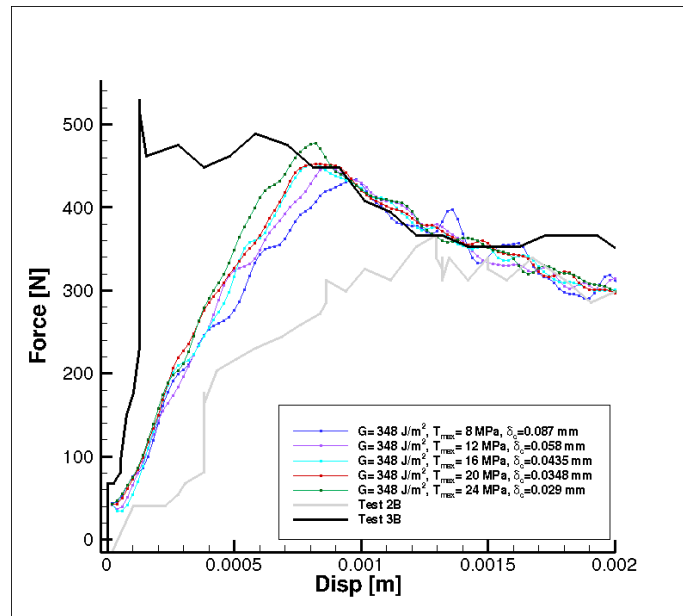


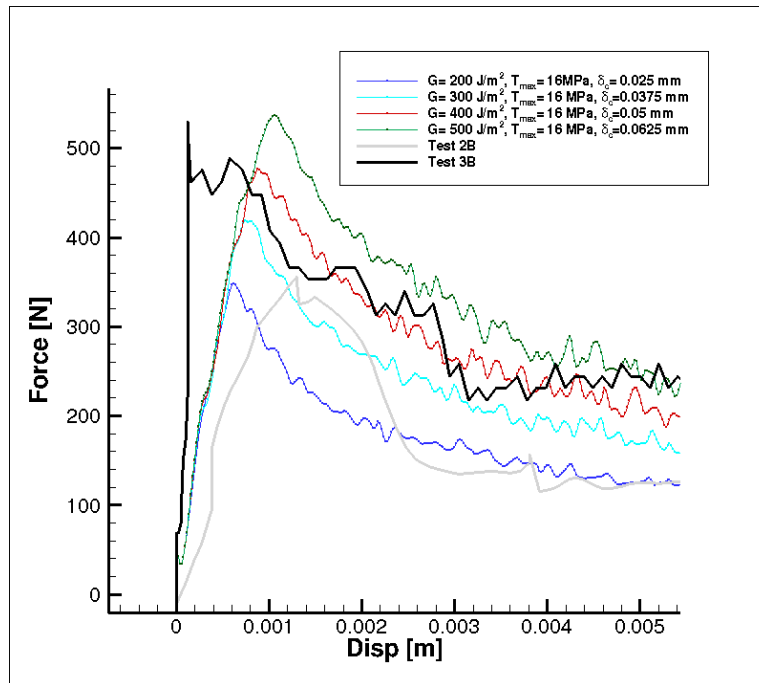
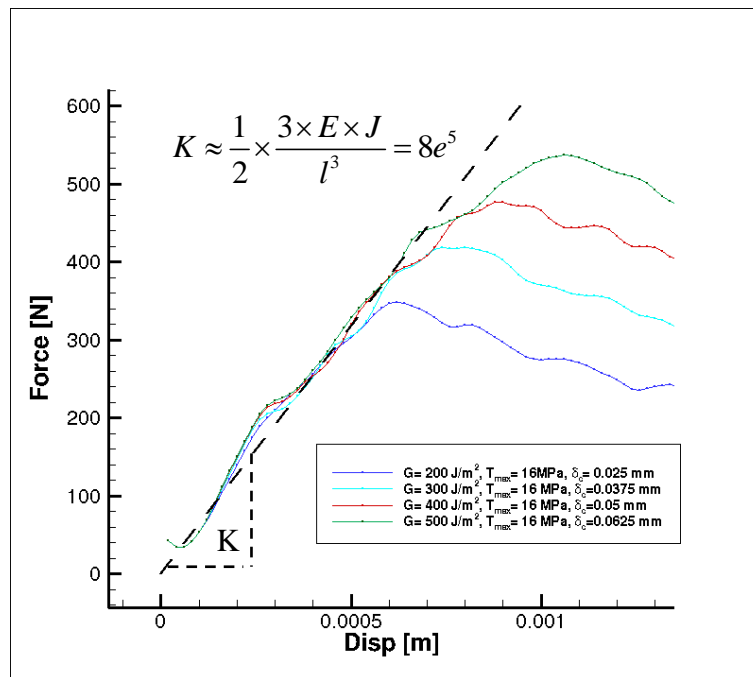
Figure 9: Influence of T_{max} on the cohesive model (FEAP)

The system shows a small dependency on T_{max} but this influence is relative small compared with the effects of G .

Effect of G

The analyses characteristics are explained in Table 2.

From Figure 10 it can be inferred that an increase of G produces an increase in the peak load admitted by the system. The initial slope for every curve (Figure 11) is independent of the value of G and matches with the bending stiffness of the beams (linear behavior).

Figure 10: Influence of G in the cohesive model (FEAP)Figure 11: Influence of G in the cohesive model – initial slope (FEAP)

d. Comparison between Abaqus and FEAP simulations

To avoid illegible graphs only one case is going to be compared, being all of them almost equal.

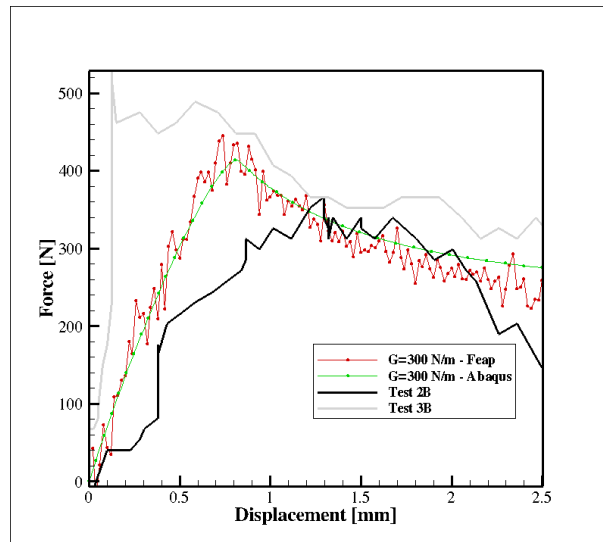


Figure 12: Results comparison for one specific case

It is possible to see an increasing discrepancy between FEAP and Abaqus after the peak. This discrepancy appears in all the results and can't be explained.

4. DISCUSSION

The first important remark is that the testing results are incomplete and can't be considered valid. The testing machine was too "robust" for the analyzed samples. To make it worst the sample rate and the precision of the load cell were too low and the calibration of the LVDT is doubtful.

Regarding the simulations a small discrepancy between Abaqus and Feap is seen after the load peak. This discrepancy cannot be explained and further debug need to be done. Even though, at the beginning of the simulations both programs show very similar results.

From both analyses it is clear that the system is more sensible to G than to T_{\max} , making the test suitable for finding the mode I fracture energy of adhesives.

5. FUTURE WORK

The first step is to redo the entire set of tests. The data is not reliable, that means that the simulation results can't be compare with the experimental results. To solve the problem using the same machine, the geometry of the specimens need to be modified.

Regarding the simulations and tests, it would be interesting to analyze the effects of plasticity in the results and the consequence of inertia effects over the behavior of the adhesive.

ACNOWLEDGMENTS

The authors of this report wish to acknowledge the following persons for its collaboration on some technical aspects: Prof. Pablo D. Zavattieri, Eng. Federico Antico and Eng. Fernando Cordisco.

REFERENCES

1. CHARACTERIZATION OF THE MODE I FRACTURE ENERGY OF ADHESIVE JOINTS, G. Steinbrecher, A. Buchman, A. Sidess, D. Sherman. International Journal of Adhesion & Adhesives 26, 2006
2. THE CALCULATION OF ADHESIVE FRACTURE ENERGIES FROM DOUBLE-CANTILEVER BEAM TEST SPECIMENS, B. Blackman, J. P. Dear, A. J. Kinloch, S. Osiyemi, Journal of materials science letters 10, 1991.
3. MACROSCOPIC MODELING OF FINE LINE ADHESION TESTS, A.A. Volinsky, J.C. Nelson, W.W. Gerberich. University of Minnesota, 1999.
4. A GRAIN LEVEL MODEL FOR THE STUDY OF FAILURE INITIATION AND EVOLUTION IN POLYCRYSTALLINE BRITTLE MATERIALS. PART I: THEORY AND NUMERICAL IMPLEMENTATION, H D. Espinosa, P D. Zavattieri. Mechanics of Materials 35, 2003.

APPENDIX 1: FEAP DISCREPANCY

The first analyses run with FEAP show an important discrepancy with the results obtained from Abaqus. This appendix show the process used to decide what software was giving the correct result and the corrections implemented.

One way to check that the correct data is being used is the “area method”:

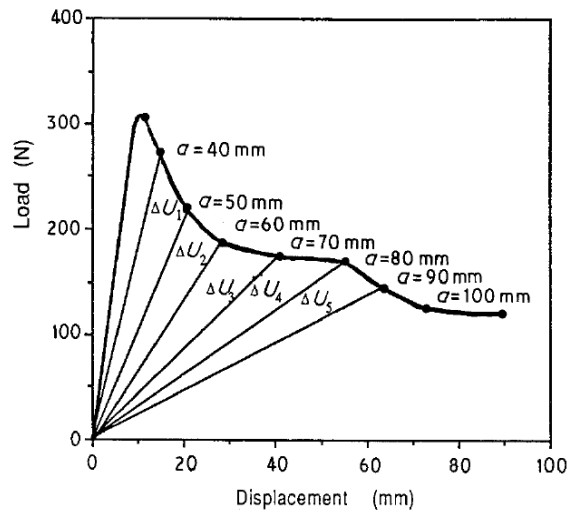


Figure 13: Typical load versus displacement curve for the DCB

$$G = \frac{\Delta U}{B \times \Delta a} \quad (6)$$

Using the output files we must recover the same “G” that we introduce as an input.

Combining the data from both graphs we get the following results.

Table 3: Values obtained from Figure 14

Point	Displacement	Force	a (crack length)
	[m]	[N]	[mm]
1	0.0005	938.7	56
2	0.0006	871.6	62
3	0.0007	810.6	68

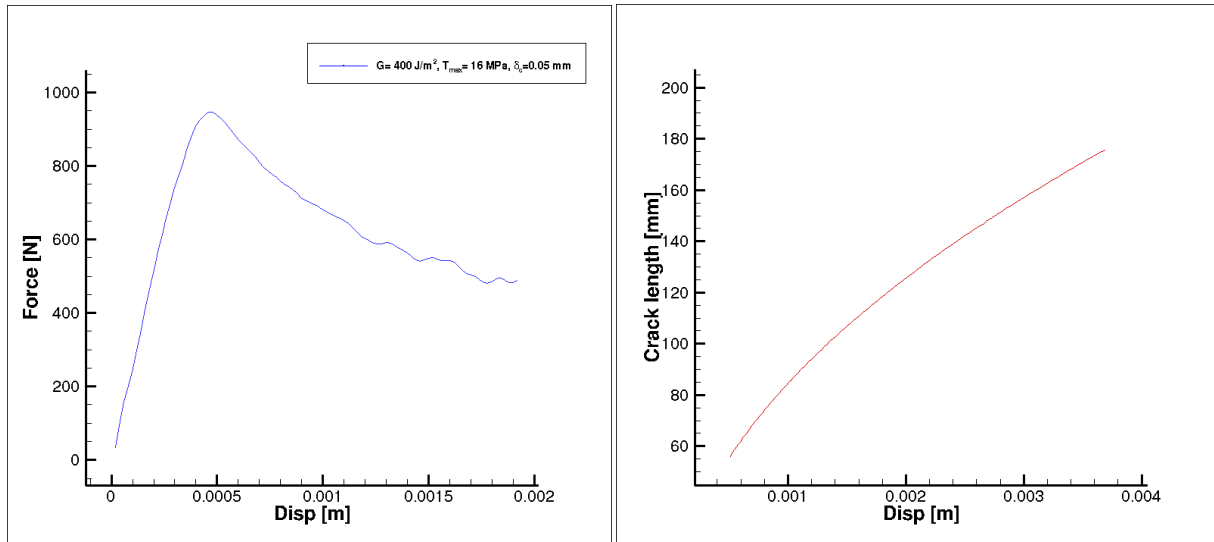


Figure 14: Left - Force vs Displacement for $G = 400 \text{ N/m}$. Right – Crack length vs Displacement for $G = 400 \text{ N/m}$ (FEAP)

Using equation (6) and approximating the area by triangles:

Table 4: Computed values for G

Points	ΔU	Δa	G
1-2	0.0637	0.006	418 N/m
2-3	0.0619	0.006	406 N/m

The results show that the cohesive law is well implemented. These allow us to focus on other inputs like material properties and BC.

After analyzing the input and output files we discovered that the reactions forces were asked to FEAP in a wrong way. This mistake was corrected and all the analyses were re-run.